oceans

MDPI

Article

Seasonal and Interannual Variations (2019–2023) in the Zooplankton Community and Its Size Composition in Funka Bay, Southwestern Hokkaido

Haochen Zhang [1], Atsushi Ooki [1,2], Tetsuya Takatsu [1] and Atsushi Yamaguchi [1,2,*]

[1] Graduate School of Fisheries Sciences, Hokkaido University, 3-1-1 Minato-cho, Hakodate 041-8611, Japan
[2] Arctic Research Center, Hokkaido University, Kita-21 Nishi-11 Kita-ku, Sapporo 001-0021, Japan
* Correspondence: a-yama@fish.hokudai.ac.jp; Tel.: +81-138-40-5631

Abstract

Funka Bay, located in southwest Hokkaido, is a vital fishing area with a shallow depth of less than 100 m. Seasonal flows of the Oyashio and Tsugaru Warm Current affect the marine environment, leading to significant changes in zooplankton communities, yet limited information is available on these variations. This study used ZooScan imaging to analyze seasonal and interannual changes in zooplankton abundance, biovolume, community structure, and size composition from 2019 to 2023. Water temperature was low in March–April and high in September–November, with chlorophyll *a* peaks occurring from February to April. Notable taxa such as Thaliacea, *Noctiluca*, and cladocerans were more common in the latter half of the year. Interannual variations included a decline in large cold-water copepods, *Eucalanus bungii* and *Neocalanus* spp., which were abundant in 2019 but decreased by 2023. Zooplankton abundance and biovolume showed synchronized seasonal changes, correlating with shifts in the Normalized Biovolume Size Spectra (NBSS) index, which measures size composition. Cluster analysis identified eight zooplankton communities, with Community A dominant from July to December across all years, while Community D was prevalent in early 2019 but was replaced in subsequent years. Community E emerged from March to April in 2021–2023. In 2019, large cold-water copepods were dominant, but from 2020 to 2023, appendicularians became the dominant group during the March–April period. The decline in large copepods is likely linked to marine heat waves, influencing yearly zooplankton community changes.

Keywords: NBSS; ZooScan; *Eucalanus bungii*; *Neocalanus* spp.; imaging analysis; Oyashio; Tsugaru Warm Current; copepods; appendicularians; marine heat wave

check for updates

Academic Editor: Santiago Hernández-León

Received: 30 May 2025
Revised: 13 July 2025
Accepted: 23 July 2025
Published: 4 August 2025

Citation: Zhang, H.; Ooki, A.; Takatsu, T.; Yamaguchi, A. Seasonal and Interannual Variations (2019–2023) in the Zooplankton Community and Its Size Composition in Funka Bay, Southwestern Hokkaido. *Oceans* **2025**, *6*, 49. https://doi.org/10.3390/oceans6030049

1. Introduction

In marine ecosystems, mesozooplankton play a crucial role in transferring energy from primary production by phytoplankton to higher trophic organisms, such as fish [1–3]. The taxonomic and size composition of mesozooplankton is vital for determining their suitability as food for fish and significantly impacts growth and mortality rates [4–6]. ZooScan is a specialized instrument that analyzes immersion samples obtained from plankton nets to gather data on the taxonomic group, size, and biovolume of mesozooplankton [7]. The size composition of the entire zooplankton community, as recorded by ZooScan, enables the calculation of the Normalized Biovolume Size Spectra (NBSS). This index serves as a measure of the efficiency of energy transfer to higher trophic organisms [8]. Theoretically,

the slope of the NBSS should be −1. A moderate slope indicates effective energy transfer to higher trophic organisms, while a slope steeper than −1 suggests limited energy transfer [9–11]. ZooScan imaging analysis has been employed to clarify seasonal and interannual changes in the population structure and size composition (NBSS) of mesozooplankton collected by plankton nets. This analysis has also been used to evaluate temporal changes in lower trophic marine ecosystems across various locations, including the Gulf of Lyon and the Bay of Villefranche in the Mediterranean Sea [12–15], the Bay of Biscay in the North Atlantic [16], off the coast of Ubatuba in Brazil [17], and the South China Sea [18].

Funka Bay, located in the southwest of Hokkaido, is a significant area for fisheries science. It has a shallow depth of less than 100 m, where walleye pollock and flatfish spawn and feed during their larval and juvenile stages [19–24]. Depending on the season, two different water masses—the Oyashio Current and the Tsugaru Warm Current—flow into Funka Bay, resulting in substantial fluctuations in the physical oceanographic environment [25,26]. The zooplankton community in Funka Bay also undergoes significant seasonal changes in response to these varying physical conditions [27–29]. Research has documented seasonal variations in the community structure of dominant zooplankton taxa in the bay [30–33]. Currently, water temperatures in Funka Bay are rising, which is believed to be a consequence of global warming. There are no longer any water masses that fit the classifications established in the 1970s [25], indicating a need for new standards for water mass classification [26]. This warming trend is expected to impact the marine ecosystem, but there is still a limited understanding of the specific changes taking place.

A study utilized ZooScan imaging analysis of plankton net samples collected over time in Funka Bay to examine seasonal and interannual changes in community structure and size composition (NBSS), as well as to evaluate temporal variations in the marine lower trophic ecosystem [34]. This research was based on plankton net samples collected monthly throughout 2019. The results indicated that the number of zooplankton individuals and their biovolume were both highest in April, with the appendicularian *Oikopleura labradoriensis*, a crucial food source for flatfish larvae [23], dominating the samples. Notably, *Noctiluca scintillans* was abundant from September to December, coinciding with the observation of the Tsugaru Warm Current. The slope of the NBSS was moderate from January to April, while it was steep from May to December, ranging from −1.09 to −0.30. This moderate NBSS slope, compared to the theoretical value of −1, suggests that energy transfer is effective for higher-trophic-level organisms, such as fish in Funka Bay [34]. Although these findings are significant, the information regarding temporal changes remains insufficient due to the limited observations conducted in just one year. Additionally, it has been reported that the flow rate of the warm Tsugaru Warm Current entering Funka Bay has increased over time [35]. Similarly, the cold Oyashio Current has undergone notable changes and exhibited a secular regime shift [36]. Furthermore, a large marine heat wave was documented in the waters off Hokkaido in the summer of 2021 [37]. These changes in the marine environment are expected to have a considerable impact on the zooplankton community in Funka Bay, but current knowledge on this topic is still limited.

This study utilized ZooScan image analysis to examine seasonal and interannual variations in zooplankton abundance, biovolume, community structure, and size composition. The data were collected 63 times at approximately one-month intervals over a five-year period from 2019 to 2023 at a fixed station in the center of Funka Bay. We employed cluster analysis and distance-based redundancy analysis (dbRDA) to explore the relationship between zooplankton community structure and environmental factors. Additionally, we calculated the NBSS (Normalized Biovolume Size Spectrum) for the zooplankton size composition to assess the efficiency of energy transfer to higher trophic levels.

2. Materials and Methods

2.1. Field Sampling

From January 2019 to December 2023, a NORPAC net with a 45 cm mouth diameter and a 100 μm mesh size, along with a flowmeter, was utilized at Station 30 (depth 95 m) in the central part of Funka Bay (Figure 1). A total of 63 collections were conducted during the daytime at approximately monthly intervals, towing the net vertically from just above the seafloor (the actual tow depth was 87 ± 2 m, mean ± standard deviation) to the sea surface. The number of collections per year varied from 9 to 19, with a mean of 12.6 ± 3.9. The net filtered a water volume of 11.9 ± 2.4 m^3, achieving an average filtration efficiency of 86%. There was a low filtering efficiency for the cases around the spring phytoplankton bloom period (February to April).

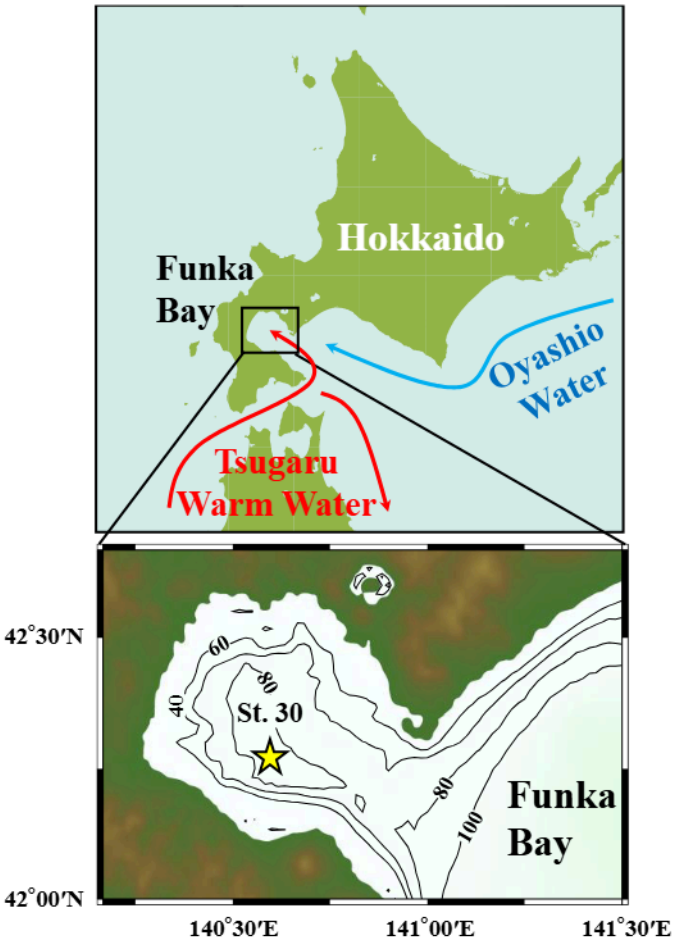

Figure 1. The Funka Bay, located on the southwestern Hokkaido Island (upper panel). Directions of the two water masses: Oyashio Water (cold current) and Tsugaru Warm Water. Station 30 in Funka Bay, the sampling station of this study (lower panel).

The collected zooplankton samples were preserved in a solution of 5% neutral formalin seawater. Simultaneously, water temperature and salinity measurements were taken using a CTD (SBE 19plus, Sea-Bird Scientific Inc., Bellevue, WA, USA). The mean temperature and salinity of the water column were calculated by averaging the data at 1 m depth intervals. Additionally, 1 L of water was collected from depths of 0, 5, 10, 20, 30, 40, 50, 60, 65, 70, 75, 80, and 85 m using either a bucket or a Niskin CTD rosette sampler. This water was then filtered through a GF/F filter, then chlorophyll a (Chl. *a*) concentrations were measured by the Welschmeyer method [38] using a fluorometer model 10-AU-005 (Turner Designs,

San Jose, CA, USA). The Chl. *a* values were averaged based on data from each layer and used as environmental data for each collection day.

2.2. ZooScan Measurement

Measurements using ZooScan (Hydrooptic Inc., L'Isle-Jourdain, France) were conducted on formalin-fixed zooplankton samples in a land-based laboratory [7]. Initially, a background image scan was performed by filling the ZooScan scanning cell with deionized water. The zooplankton samples were then divided into subsamples ranging from 1/3 to 1/90, depending on the total amount of the sample. These subsamples were individually scanned. The resulting images were processed and segmented into individual images using ZooProcess software (v7.28, PIQv (Quantitative Imaging Platform) of Institute de La Mer de Villefranche (IMEV), Villefranche sur Mer, France). The images were digitized at a resolution of 2400 dpi, with one pixel representing 10.6 µm. Finally, the images were uploaded to the Ecotaxa website, where the semi-automatic identification of taxa was conducted online.

The identified taxonomic groups and species included large copepods such as *Eucalnus bungii*, *Metridia pacifica*, and *Neocalanus* spp.; various other Copepoda; Amphipoda; Appendicularia; Chaetognatha; Cladocera; Cnidaria; Euphausiacea; *Limacina*; Thaliacea; Bivalvia larvae; Echinodermata larvae; Polychaeta larvae; and *Noctiluca scintillans*. Detritus, which is non-living, is not included in the analysis.

The size of each zooplankton was determined by measuring the excluded area, which refers to the area of the object captured in the scanned image, excluding everything except for the zooplankton [7]. The equivalent spherical diameter (ESD, in micrometers) was calculated using the following formula:

$$\text{ESD} = 2 \times \sqrt{\frac{\textit{Area excluded}}{\pi}} \tag{1}$$

The volume ($\mu m^3 \cdot ind.^{-1}$) of each zooplankton was then calculated using this formula:

$$\text{Volume} = \frac{4}{3}\pi\left(\frac{ESD}{2}\right)^3 \tag{2}$$

2.3. Data Analysis

The NBSS analysis was conducted based on the zooplankton size composition obtained through ZooScan [12–18]. A net with a mesh size of 100 µm was utilized in this study. Consequently, data with an equivalent spherical diameter (ESD) of less than 0.2 mm were excluded from the NBSS calculations to prevent underestimating biovolumes for smaller sizes [34]. The NBSS data were calculated by integrating the biovolumes ($mm^3 \cdot m^{-3}$) for ESDs ranging from 0.2 to 5.0 mm, as measured by ZooScan, in increments of 0.05 mm.

The *x*-axis of the NBSS graph represents the logarithmic transformation of the biovolumes for each size class (X: $\log_{10}$ of zooplankton biovolume [mm^3]), while the *y*-axis represents the logarithmic transformation of the biovolumes for each size class divided by the difference in biovolume between adjacent size classes (Δbiovolume [mm^3]) (Y: $\log_{10}$ of zooplankton biovolume [$mm^3 \cdot m^{-3}$]/Δbiovolume [mm^3]).

Using the MS Excel Solver function, we performed an approximate linear regression with the X-axis and Y-axis values to derive the linear equation for the NBSS:

$$Y = aX + b \tag{3}$$

In this equation, 'a' represents the slope of the NBSS, and 'b' indicates the intercept. We also created a scatter plot to illustrate the relationship between the slope and the intercept of the NBSS, with the *y*-axis depicting the slope and the *x*-axis depicting the intercept.

To clarify the seasonal changes in zooplankton community structure, we conducted a cluster analysis using abundance data from all samples. The abundance data for each zooplankton taxonomic group in each sample (X: ind.·m^{-3}) was transformed into fourth roots ($\sqrt[4]{X}$) to reduce the bias of abundant species. We performed cluster analysis by connecting the Bray–Curtis similarity index with the average linkage method. Additionally, a distance-based redundancy analysis (dbRDA) was performed. To evaluate the differences in abundance and environmental variables among the zooplankton communities identified in the cluster analysis, we utilized one-way ANOVA. All statistical analyses were conducted using Primer7 (with PERMANOVA+, PRIMER-e, Auckland, New Zealand) and StatView software (ver. 5.0.1, SAS Institute Inc., Cary, NC, USA).

3. Results

3.1. Hydrography

The seasonal variations in water temperature, salinity, Chl. *a*, and the temperature–salinity (T-S) diagrams at Funka Bay Station 30 from 2019 to 2023 are illustrated in Figure 2. Throughout this period, the mean water column temperature ranged from 2.1 to 20.5 °C. The lowest water temperatures, approximately 2 to 4 °C, were recorded in March and April (Figure 2A), while the highest temperatures were observed from September to November. In terms of salinity, the mean water column values varied between 32.2 and 34.0, with the lowest salinity levels occurring from May to July and the highest levels noted in December and January.

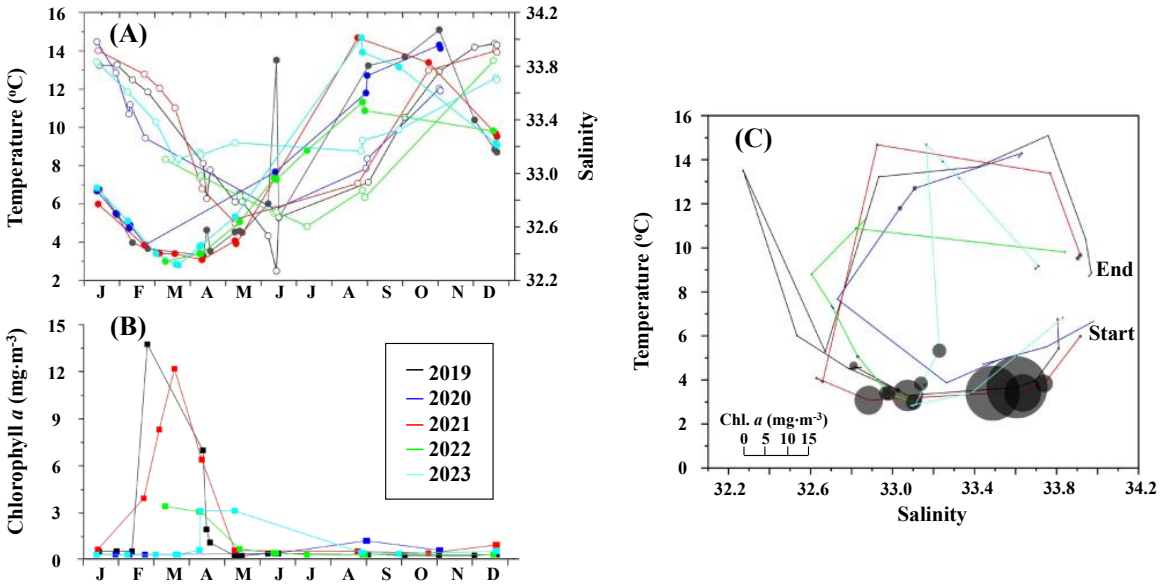

Figure 2. (**A**) Seasonal changes in mean temperature (solid symbols) and salinity (open symbols) at St. 30 in central Funka Bay from 2019 to 2023. (**B**) Seasonal changes in mean chlorophyll *a* at the station. (**C**) T-S diagram showing the mean chlorophyll *a* with the size of the circles. The different line colors in each panel correspond to the various years indicated in the legend box located in the open space of (**B**).

The mean concentration of Chl. *a* in the water column ranged from 0.1 to 13.5 mg·m^3, with seasonal peaks occurring between February and April, coinciding with the spring phytoplankton bloom (Figure 2B). In the T-S diagram, a distinct seasonal pattern was typically observed each year. This pattern started in the lower right corner, where temperatures

were low and salinity was high. It then moved to the lower left (low temperature and low salinity), followed by an increase in temperature that transitioned to the upper left (high temperature and low salinity), and finally to the upper right (high temperature and high salinity) (Figure 2C).

3.2. Zooplankton Abundance, Biovolume, and NBSS

The seasonal and interannual variations in the abundance and biovolume of each zooplankton taxon at Funka Bay Station 30 from 2019 to 2023 are illustrated in Figure 3. Each zooplankton taxon displayed distinct seasonal patterns; for instance, Thaliacea, *Noctiluca*, and Cladocera were more abundant in the latter half of the year. Interannual changes were observed in large cold-water copepods such as *E. bungii* and *Neocalanus* spp. Both of these taxa were more prevalent in 2019 but showed a decline in abundance by 2023.

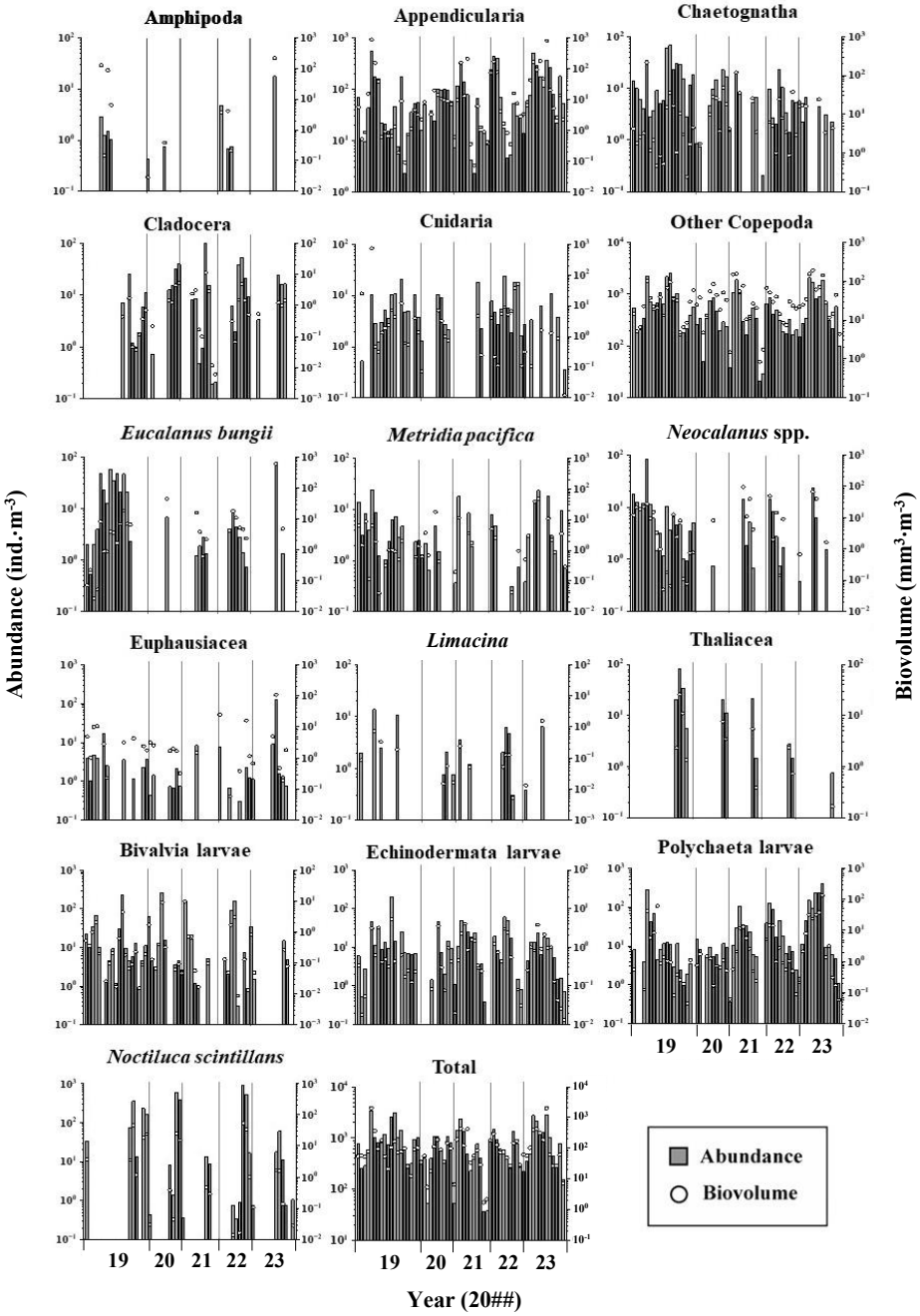

Figure 3. Seasonal and yearly changes in abundance and biovolume of each zooplankton taxon or species at St. 30 in central Funka Bay from 2019 to 2023.

The seasonal and interannual variations in the zooplankton abundance and their biovolume, along with the slope and intercept of the NBSS throughout the survey period, are presented in Figure 4. The zooplankton abundance and their biovolume exhibited seasonal and interannual changes that were closely synchronized; higher biovolumes corresponded with a greater abundance (Figure 4A). Additionally, the seasonal and interannual changes in the slope and intercept of the NBSS, which served as an index of the zooplankton size composition, also displayed synchronization. Specifically, the intercepts were higher when the slope of the NBSS was less steep (Figure 4B).

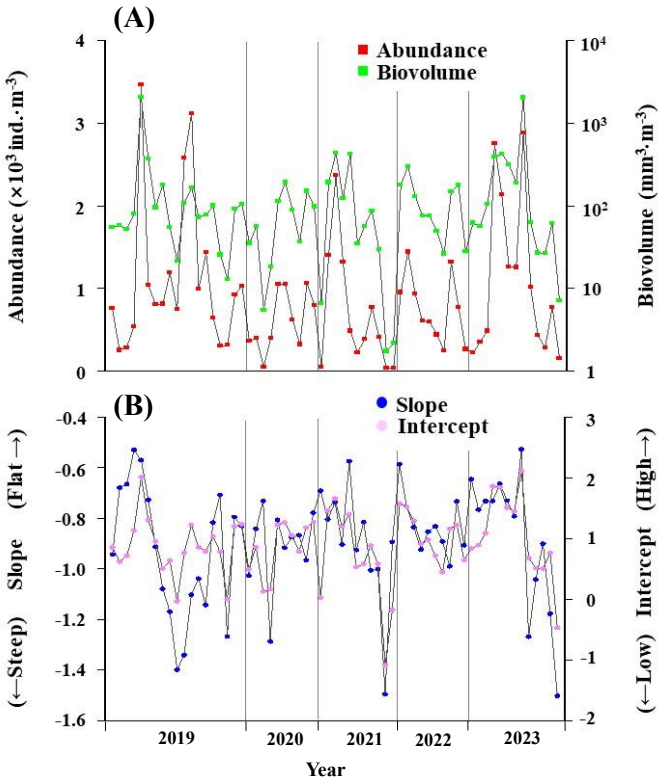

Figure 4. (**A**) Seasonal and yearly changes in total zooplankton abundance and biovolume (upper panel) and (**B**) slope and intercept of the Normalized Biovolume Size Spectrum (NBSS) at St. 30 in central Funka Bay from 2019 to 2023.

3.3. Zooplankton Community

Cluster analysis was conducted on the zooplankton population data, resulting in the classification of each collection date into eight distinct clusters (A–H) (Figure 5A). Regarding seasonal variations, Community A, which was predominant during the latter half of the year (July–December), was consistently observed across all five years of the survey and was notably characteristic (Figure 5B). In terms of temporal changes, Community D, which appeared in the first half of the year (January–June) in 2019, was subsequently replaced by Communities E, F, G, and H from 2020 to 2023 (Figure 5B). Community E was also recorded in March and April from 2021 to 2023. The dbRDA (distance-based redundancy analysis) diagram demonstrated clear distinctions between the locations of the zooplankton communities, highlighting significant seasonality. The plot positions formed a circular pattern within each year, as illustrated in the T-S diagram mentioned earlier (Figure 5C). The dbRDA map indicated a significant relationship between the environmental factors of water temperature and salinity, with Community A situated in the direction of high temperature and high salinity.

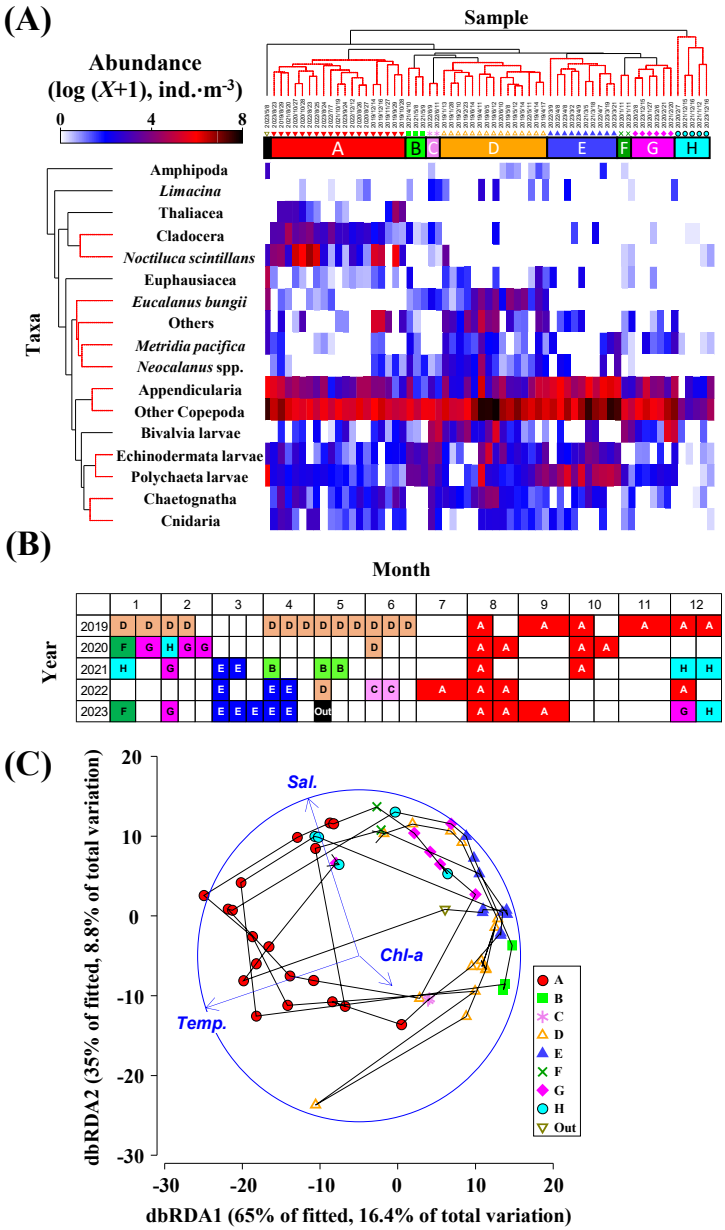

Figure 5. (**A**) Results of the cluster analysis based on zooplankton abundance at St. 30 in central Funka Bay from 2019 to 2023. Taxonomic and sample categories were arranged for the vertical and horizontal axes, respectively. Differences in color indicate abundance values. (**B**) Seasonal and yearly occurrences of eight groups (group A–H). (**C**) dbRDA plots of the groups with environmental parameters. The arrowhead directions indicate high values of the environmental parameters (Temp.: temperature, Sal.: salinity, Chl-a: chlorophyll *a*).

The mean abundances of each taxonomic group within the zooplankton communities are presented in Table 1. Among the eight communities studied, Cladocera, Thaliacea, and *Noctiluca* were particularly abundant in Community A, which was observed in the latter half of the year (July–December), indicating a clear seasonal change. In contrast, during the first half of the year (January–June), notable interannual changes were recorded. Community D, observed in 2019, featured a high abundance of large cold-water Copepoda, such as *E. bungii* and *Neocalanus* spp. Meanwhile, communities E, F, G, and H, which were observed from 2020 to 2023, displayed a significantly lower abundance of these large cold-water copepods. Community E, noted collectively in March and April of 2021–2023, was distinguished by a high abundance of Appendicularia.

Table 1. Mean abundance of each zooplankton taxon and the species of eight zooplankton groups (A–H) identified at St. 30 in central Funka Bay from 2019 to 2023 (cf. Figure 5A). Parentheses indicate the number of samples included for each group. Differences between groups were tested by one-way ANOVA. NS: not significant, *: $p < 0.05$, **: $p < 0.01$, ***: $p < 0.001$.

Taxa/Species	Mean Abundance (Ind.·m^{-3})								One-Way ANOVA
	A (19)	B (3)	C (2)	D (15)	E (10)	F (2)	G (6)	H (5)	
Amphipoda	0	0	0.38	0.54	0.48	0.22	0	0	NS
Appendicularia	64.87	28.32	10.97	87.09	271.02	14.88	77.64	16.58	NS
Chaetognatha	10.51	0	16.81	17.19	5.12	3.30	1.28	0.33	NS
Cladocera	23.12	3.28	4.01	0.48	1.15	0	0.12	0.08	**
Cnidaria	6.95	0	14.85	4.25	2.48	1.99	0	0.07	NS
Other Copepoda	349.05	263.73	247.99	941.58	1057.37	205.26	556.21	47.51	***
Eucalanus bungii	0.52	1.96	6.30	21.97	0	0	0	0	*
Metridia pacifica	0.78	3.44	0	5.60	4.92	0.84	6.19	0.35	NS
Neocalanus spp.	1.15	7.17	1.21	12.06	5.18	0.19	0	0	***
Euphausiacea	1.00	2.81	0	2.50	1.67	0.79	0.24	0	NS
Limacina	0.20	0.40	5.34	2.07	0.63	0.19	0.59	0	NS
Thaliacea	10.52	0	0	0	0	0	0	0	NS
Bivalvia larvae	4.05	0.71	124.57	30.20	4.13	49.80	74.71	1.03	**
Echinodermata larvae	6.70	22.50	53.94	26.00	19.13	0	3.02	0.44	**
Polychaeta larvae	5.85	30.56	31.71	31.89	113.39	8.34	8.29	0.28	**
Noctiluca scintillans	171.76	0	0.54	2.23	0	0.60	0	0.28	*
Others	26.10	0.96	0	30.84	2.13	4.66	2.39	0	NS
Total	683.15	365.84	518.62	1216.48	1488.78	291.04	730.69	66.95	NS

The mean temperature, salinity, Chl. *a*, total zooplankton abundance, biovolume, NBSS slope, and intercept for each zooplankton community are summarized in Table 2. Community A, observed in the second half of the year, was characterized by a low abundance and biovolume, a low NBSS intercept, and a relatively steep slope. In addition, two communities that exhibited distinct changes over time—Community D (2019) and Community E (2021–2023), both observed in the first half of the year (January to June)—had high mean values for water column Chl. *a*, total zooplankton abundance, and biovolume. The main differences between these two communities were in the slope and intercept of the NBSS; Community E had a higher intercept (1.50 for Community E compared to 0.91 for Community D) and a moderate slope (−0.75 for Community E compared to −0.93 for Community D).

Based on data collected on all dates, there was a highly significant positive relationship between biovolume and the number of individuals, indicated by the slope and intercept of the NBSS ($r^2 = 0.441$–0.761, $p < 0.0001$) (Figure 6). Among the zooplankton communities that exhibited these changes over time, Community D, observed in 2019, often fell below the regression line relating the abundance to the biovolume. This community was characterized by a low biovolume relative to the abundance. In contrast, Community E, observed from 2021 to 2023, was consistently plotted above the regression line and was characterized by a high biovolume per abundance (Figure 6A). Regarding the NBSS, the slope of Community D in 2019 showed considerable variation between samples. In comparison, the slope of Community E from 2021 to 2023 displayed a moderate slope and a higher intercept across all samples (Figure 6B).

Table 2. Mean values of the environmental/zooplankton parameters of eight zooplankton groups (A–H) identified at St. 30 in central Funka Bay from 2019 to 2023 (cf. Figure 5A). Parentheses indicate the number of samples included for each group. Differences between groups were tested by one-way ANOVA. NS: not significant, ****: $p < 0.0001$.

Parameters	Groups								One-Way ANOVA
	A (19)	B (3)	C (2)	D (15)	E (10)	F (2)	G (6)	H (5)	
Temperature (°C)	12.29	3.70	7.31	5.50	3.32	6.75	5.40	7.79	****
Salinity	33.37	32.72	32.71	33.02	33.20	33.91	33.60	33.77	****
Chl. *a* (mg m^{-3})	0.50	2.55	0.46	2.13	3.50	0.36	0.99	0.71	NS
Total zooplankton abundance (ind.·m^{-3})	683.2	365.8	518.6	1216.5	1488.8	291.0	730.7	67.0	NS
biovolume (mm^3·m^{-3})	73.4	169.8	62.2	240.3	258.3	48.4	82.7	4.6	NS
NBSS									
Intercept	0.84	0.84	0.85	0.91	1.50	0.66	0.89	−0.32	****
Slope	−0.94	−0.77	−0.84	−0.93	−0.75	−0.84	−0.95	−1.06	NS

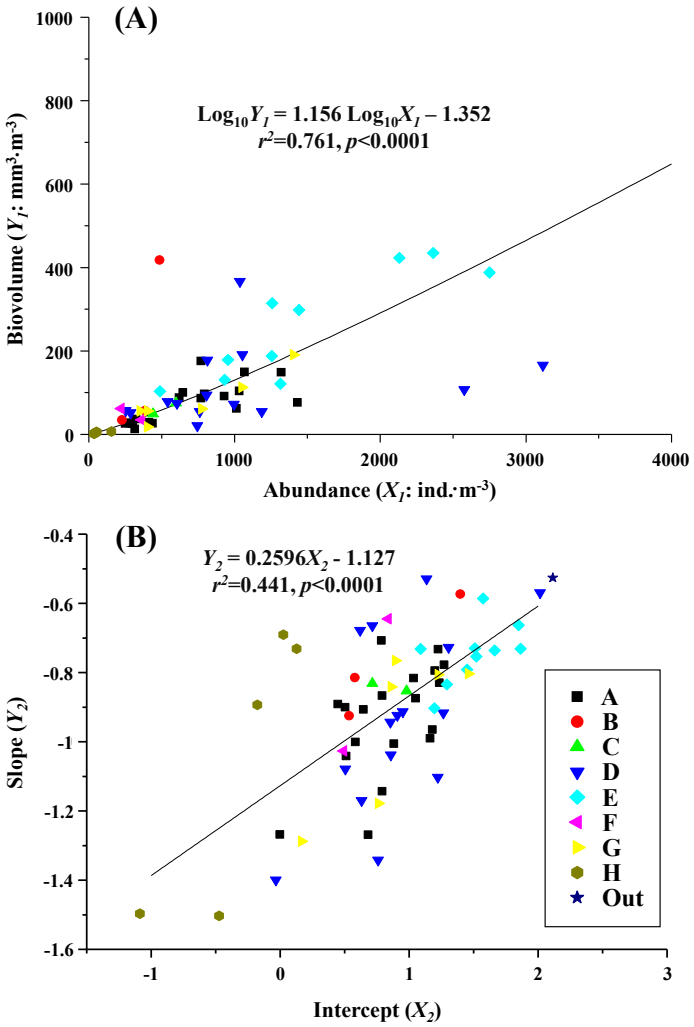

Figure 6. (**A**) Relationship between biovolume and abundance and (**B**) NBSS slope and intercept of all whole zooplankton samples collected at St. 30 in central Funka Bay from 2019 to 2023. Significant regressions were present between them. Differences in symbols indicate differences in eight zooplankton groups (cf. Figure 5A).

4. Discussion

4.1. Zooplankton Community

The data from 2019 in this study are consistent with those presented in reference [34]. However, by combining samples collected at fixed points from 2020 to 2023, we were able to evaluate changes over time that single-year observations could not reveal. The results of this study differ from those of [34] in three key ways: (1) We discovered a seasonal community (Community A) that showed no change over time during the latter half of the year (July–December) when water temperatures were high. (2) In contrast, the community present in the first half of the year (January–June), when water temperatures were low, changed over time. In 2019, this community was dominated by large Copepoda (Community D), while from 2021 to 2023, it shifted to being dominated by Appendicularia (Community E). (3) Additionally, we found that the energy transfer to higher organisms was more consistent over time from 2021 to 2023 compared to 2019. Each of these findings will be explained in detail in separate chapters below.

4.2. Zooplankton Community Observed During Warm Period

The zooplankton community observed during the warm period from July to December (referred to as Community A) was consistently present across all five years of the survey (Figure 5B). The dominant taxa in this community were *Noctiluca*, Cladocera, and Thaliacea (Table 1). Notably, previous studies on seasonal changes in the zooplankton fauna of Funka Bay did not report the dominance of *Noctiluca* [29], making this the first documentation of its prevalence in seasonal studies from 2019 to 2023. *Noctiluca* is a species commonly found in warmer waters, such as those influenced by the Kuroshio Current and the Tsushima Warm Current [39–41]. In this study, Community A, where *Noctiluca* was abundant, was associated with the highest average water column temperature of 12.3 °C compared to other communities (Table 2). Recent reports indicate that the flow rate of the Tsugaru Warm Current, which also enters Funka Bay, has increased in recent years [35]. The water mass classification criteria for Funka Bay have become outdated and no longer align with the classifications established in the 1970s [25]. Therefore, a revised classification system that modifies the temperature ranges on the T–S diagram is required [26]. In the context of ongoing global warming, the emergence of warm-water *Noctiluca* during this high-temperature period is significant, highlighting its impact on the zooplankton community in Funka Bay.

Research on the distribution of marine Cladocera in Japanese waters includes a study examining seasonal changes in their abundance in the water column of the Seto Inland Sea and the presence of resting eggs in the bottom sediment [42]. Additionally, another study has focused on the seasonal variations in both the vertical distribution and the number of individuals in Toyama Bay, located in the Sea of Japan [43]. It has been observed that Cladocera are only present in Toyama Bay during the relatively warm water temperatures of mid-March to early December [43]. They do not appear when water temperatures drop from mid-December to early March [43]. This observation aligns with findings from Funka Bay, situated in southwestern Hokkaido, where Cladocera are frequently found during the warm season, coinciding with the influx of Tsugaru Warm Current water from the Sea of Japan (Tables 1 and 2).

There have been no reports regarding the dominance of Thaliacea in Funka Bay. In this study, Thaliacea were only observed in the high-temperature Community A and were not found in other communities (see Table 1). In the Sea of Japan, salps belonging to the Thaliacea are often dominant, and their presence has been reported to cause damage to fisheries [44,45]. The limited appearance of Thaliacea in this study, restricted to the high-temperature Community A, may be interpreted as a result of increased salp populations in

the Sea of Japan being transported by the Tsugaru Warm Current. Recent reports indicate that the flow rate of the Tsugaru Warm Current, which moves from the Sea of Japan across the Tsugaru Strait, has increased in recent years [35]. This phenomenon is thought to support the regular presence of the zooplankton community (Community A) in Funka Bay during the high-temperature season, typically from July to December.

4.3. Interannual Changes in Zooplankton Community

Observations of zooplankton communities in Funka Bay over a five-year period have revealed changes in these communities during the cold period from January to June. In 2019, the communities were dominated by large cold-water Copepoda, such as *E. bungii* and *Neocalanus* species (Community D). However, from 2020 to 2023, communities E, F, G, and H exhibited a marked decline in the abundance of these large cold-water Copepoda. Notably, between March and April from 2021 to 2023, the communities were primarily dominated by Appendicularia (Community E) (see Figure 5B and Table 1). Additionally, a separate study examining changes in the hydrological environment in Funka Bay and the Tsugaru Strait from February to April between 2010 and 2018 found significant alterations in the water mass structure over time and identified a regime shift [36]. This suggests that while changes during the high-water-temperature period are minimal, the low-water-temperature period experiences notable shifts in the hydrological environment.

Various studies have indicated that the population of large copepods, specifically three species from the genus *Neocalanus* (*N. cristatus*, *N. flemingeri*, and *N. plumchrus*) along with *E. bungii* in the western subarctic Pacific, has undergone changes from the 1960s to the 1990s [46–48]. The abundance of *N. flemingeri* and *N. plumchrus* is believed to be influenced by primary production levels, which are affected by the ocean's thermal stratification and the timing of the spring phytoplankton bloom [46]. Additionally, significant climatic regime shifts, particularly those observed in 1976/77 and 1989/90, play a crucial role in affecting the biomass of *Neocalanus* spp. Predation pressure from pelagic fish, such as the Japanese sardine, is also an important factor [47]. Moreover, studies have shown that *Neocalanus* copepods reproduce in deeper waters and only produce recruits at the surface. In contrast, *E. bungii* reproduces at the surface and also generates recruits, indicating that the mechanisms driving interannual changes in *E. bungii* differ from those in the *Neocalanus* species [48].

In the summer of 2021, a large-scale marine heatwave was reported in the waters off Hokkaido [37]. During this time, the abundance of pelagic fish, such as Pacific saury, decreased, whereas the abundance of Japanese sardines increased [49,50]. These changes in fish populations coincided with a shift in the zooplankton community in Funka Bay. Specifically, there was a transition from a community dominated by large Copepoda (such as *E. bungii* and *Neocalanus* spp.) to one dominated by Appendicularia during the low-water-temperature period. It is believed that the decline in the abundance of large copepods in the Oyashio water, which flows into Funka Bay during this time, has influenced this change in the zooplankton community.

The dominant Appendicularia species in the zooplankton community (Community E) observed in Funka Bay during the low-water-temperature period from 2021 to 2023 is believed to be the cold-water species *Oikopleura labradoriensis* [31,33]. In Funka Bay, Appendicularia, including the cold-water species *Fritillaria borealis* and *O. labradoriensis*, are particularly abundant, especially in the winter waters of Funka Bay and Oyashio [31,33]. In the subarctic zone of the Northern Hemisphere, Appendicularia exhibit high filtration rates and productivity, and their discarded houses play a significant role in the vertical transport of materials [51–54]. Studies indicate that Appendicularia, particularly *O. labradoriensis*, are an important food source for larval flatfish and flounder in Funka Bay from January

to May [23,55]. It is suggested that during spring, Appendicularia contribute significantly to material circulation and food webs by rapidly transferring the products of the spring phytoplankton bloom to higher trophic levels.

Thus, zooplankton communities in Funka Bay exhibited yearly variations during the low-water-temperature period from January to June. This is believed to be due to a lower abundance of large copepods in the Oyashio water, which flows into Funka Bay, between 2021 and 2023. Consequently, this decline allowed Appendicularia to thrive and dominate by taking advantage of the surplus production resulting from the spring phytoplankton bloom.

4.4. Energy Transfer to Higher Trophic Levels via Zooplankton

The NBSS of a zooplankton community serves as an indicator of the efficiency of energy transfer to higher organisms, such as fish [11,17,56,57]. A slope of −1 in the NBSS indicates a stationary zooplankton community. If the slope is steeper than −1, it suggests low energy transfer efficiency, while a slope more moderate than −1 signifies high energy transfer efficiency [9]. In this study, among the observed zooplankton communities, Community E had the flattest NBSS slope at −0.75 during the low-water-temperature period from January to June in 2021–2023 (Table 2).

In contrast, during the same low-water-temperature period in 2019, Community D exhibited a much steeper average NBSS slope of −0.93 (Table 2), along with significant variability in the NBSS slope between samples (Figure 6B) and a low biovolume per abundance observed (Figure 6A). Conversely, Community E observed in 2021–2023 demonstrated a high biovolume per abundance (Figure 6A), a moderate NBSS slope (Figure 6B), and the highest intercept (Table 2). These findings suggest that the low-water-temperature period from January to June in 2021–2023 facilitated better energy transfer to higher trophic organisms compared to 2019.

In Funka Bay, during the period of low water temperatures, a well-known pathway for transferring spring phytoplankton production to higher organisms involves small zooplankton. Specifically, this transfer occurs through the feeding of walleye pollock larvae on the reproduced nauplii of small Copepoda, such as *Oithona* and *Pseudocalanus* [20–22,24]. Furthermore, the consumption of Appendicularia *O. labradoriensis* by larval flatfish and flounders is considered a crucial pathway for transferring nutrients to higher organisms [23]. During the warm period from July to December, Communities A and H noted that the NBSS slope was steep while the intercept was low. This phenomenon is believed to be caused by a decline in the abundance of small-sized species, as well as a low efficiency of energy transfer to higher trophic organisms. However, the mean slopes of the NBSS for each zooplankton community in Funka Bay were generally more moderate than −1 (Table 2). This indicates that transfer efficiency in Funka Bay exceeds that of typical marine environments year-round. In fact, during the spring phytoplankton bloom period, primary production in Funka Bay can reach a maximum of 1.4 $g \cdot C \cdot m^{-2} \cdot day^{-1}$, making it one of the most productive marine areas in the world [58]. The zooplankton community (Community E) exhibited a high NBSS intercept and a moderate slope during the low-water-temperature period from 2021 to 2023. This community is believed to facilitate the efficient transfer of products from the spring phytoplankton bloom to higher organisms, such as fish.

5. Conclusions

Observations of zooplankton communities in Funka Bay over a five-year period revealed that the same communities were consistently present each year during the warm-water period (July–December), showing no interannual changes. In contrast, the communities observed during the cold-water period (January–June) exhibited significant interannual

variations. For instance, large cold-water copepods dominated in 2019, but from 2020 to 2023, these large copepods became scarce. Notably, from March to April in the years 2021 to 2023, the communities shifted to being predominantly composed of Appendicularia. From the perspective of the zooplankton size class, the communities dominated by Appendicularia during the cold-water periods of 2021 to 2023 showed high NBSS intercepts and moderate NBSS slopes. This suggests that Appendicularia play a crucial role in material flux and contribute to a high energy transfer efficiency to higher trophic levels, such as flatfish larvae, within marine food webs.

Author Contributions: Conceptualization, H.Z. and A.Y.; methodology, A.O. and T.T.; software, H.Z.; validation, H.Z. and A.Y.; formal analysis, H.Z.; investigation, A.O. and T.T.; resources, A.O. and T.T.; data curation, A.Y.; writing—original draft preparation, H.Z.; writing—review and editing, A.Y.; visualization, H.Z.; supervision, A.Y.; project administration, A.Y.; funding acquisition, A.Y. All authors have read and agreed to the published version of the manuscript.

Funding: Part of this study was supported by Grant-in-Aid for Challenging Research (Pioneering) 20K20573, Scientific Research 22H00374 (A) from the Japan Society for the Promotion of Science (JSPS).

Institutional Review Board Statement: Not applicable.

Informed Consent Statement: Not applicable.

Data Availability Statement: Data will be available from request to the corresponding author.

Acknowledgments: We thank the captains, officers, crews, and researchers onboard the T/S *Ushio-Maru* for their great efforts during field sampling.

Conflicts of Interest: The authors declare no conflicts of interest.

References

1. Thorpe, R.B. We need to talk about the role of zooplankton in marine food webs. *J. Fish Biol.* **2024**, *105*, 444–458. [CrossRef] [PubMed]
2. Bisinicu, E.; Harcota, G.E. Baseline assessment of Black Sea food web integrity using a zooplankton-based approach under the marine strategy framework directive. *J. Mar. Sci. Eng.* **2025**, *13*, 713. [CrossRef]
3. Bisinicu, E.; Harcota, G.-E.; Lazar, L. Interactions between environmental factors and the mesozooplankton community from the Romanian Black Sea waters. *Tur. J. Zool.* **2023**, *47*, 202–215. [CrossRef]
4. Badouvas, N.; Tsagarakis, K.; Somarakis, S.; Karachle, P.K. Feeding habits and prey composition of six mesopelagic fish species from an isolated Central Mediterranean Basin. *Fishes* **2025**, *10*, 182. [CrossRef]
5. Bișinicu, E.; Harcotă, G.-E.; Lazăr, L.; Niță, V.; Țoțoiu, A.; Țiganov, G. Fish abundance and mesozooplankton resource: A study on *Sprattus sprattus* (Linnaeus, 1758) (Actinopterygii: Clupeidae) in the Romanian Black Sea Waters. *Acta Zool. Bulg.* **2024**, *76*, 215–224. [CrossRef]
6. Wang, Y.-C.; Lee, M.-A.; He, J.-S. Feeding habits of *Mene maculata* (Teleostei: Menidae) in the southwestern waters of Taiwan, western Pacific Ocean. *Fishes* **2025**, *10*, 182. [CrossRef]
7. Gorsky, G.; Ohman, M.D.; Picheral, M.; Gasparini, S.; Stemmann, L.; Romagnan, J.B.; Cawood, A.; Pesant, S.; García-Comas, C.; Prejger, F. Digital zooplankton image analysis using the ZooScan integrated system. *J. Plankton Res.* **2010**, *32*, 285–303. [CrossRef]
8. Vandromme, P.; Stemmann, L.; García-Comas, C.; Berline, L.; Sun, X.; Gorsky, G. Assessing biases in computing size spectra of automatically classified zooplankton from imaging systems: A case study with the ZooScan integrated system. *Methods Oceanogr.* **2012**, *1–2*, 3–21.
9. Sprules, W.G.; Munawar, M. Plankton size spectra in relation to ecosystem productivity, size, and perturbation. *Can. J. Fish. Aquat. Sci.* **1986**, *43*, 1789–1794. [CrossRef]
10. Moore, S.K.; Suthers, I.M. Evaluation and correction of subresolved particles by the optical plankton counter in three Australian estuaries with pristine to highly modified catchments. *J. Geophys. Res.* **2006**, *111*, C05S04. [CrossRef]
11. Zhou, M. What determines the slope of a plankton biomass spectrum? *J. Plankton Res.* **2006**, *28*, 437–448. [CrossRef]
12. Espinasse, B.; Carlotti, F.; Zhou, M.; Devenon, J.L. Defining zooplankton habitats in the Gulf of Lion (NW Mediterranean Sea) using size structure and environmental conditions. *Mar. Ecol. Prog. Ser.* **2014**, *506*, 31–46. [CrossRef]

13. Romagnan, J.-B.; Legendre, L.; Guidi, L.; Jamet, J.-L.; Jamet, D.; Mousseau, L.; Pedrotti, M.-L.; Picheral, M.; Gorsky, G.; Sardet, C.; et al. Comprehensive model of annual plankton succession based on the whole-plankton time series approach. *PLoS ONE* **2015**, *10*, e0119219. [CrossRef]
14. Romagnan, J.-B.; Aldamman, L.; Gasparini, S.; Nival, P.; Aubert, A.; Jamet, J.-L.; Stemmann, L. High frequency mesozooplankton monitoring: Can imaging systems and automated sample analysis help us describe and interpret changes in zooplankton community composition and size structure-An example from a coastal site. *J. Mar. Syst.* **2016**, *162*, 18–28. [CrossRef]
15. Feuilloley, G.; Fromentin, J.M.; Saraux, C.; Irisson, J.O.; Jalabert, L.; Stemmann, L. Temporal fluctuations in zooplankton size, abundance, and taxonomic composition since 1995 in the North Western Mediterranean Sea. *ICES J. Mar. Sci.* **2022**, *79*, 882–900. [CrossRef]
16. Vandromme, P.; Nogueira, E.; Huret, M.; Lopez-Urrutia, Á.; González-Nuevo, G.; Sourisseau, M.; Petitgas, P. Springtime zooplankton size structure over the continental shelf of the Bay of Biscay. *Ocean Sci.* **2014**, *10*, 821–835. [CrossRef]
17. Marcolin, C.R.; Gaeta, S.; Lopes, R.M. Seasonal and interannual variability of zooplankton vertical distribution and biomass size spectra off Ubatuba, Brazil. *J. Plankton Res.* **2015**, *37*, 808–819. [CrossRef]
18. Zhang, W.; Sun, X.; Zheng, S.; Zhu, M.; Liang, J.; Du, J.; Yang, C. Plankton abundance, biovolume, and normalized biovolume size spectra in the northern slope of the South China Sea in autumn 2014 and summer 2015. *Deep-Sea Res. II* **2019**, *167*, 79–92. [CrossRef]
19. Kamba, M. Feeding habits and vertical distribution of walleye pollock, *Theragra chalcogramma* (Pallas), in early life stage in Uchiura Bay, Hokkaido. *Res. Inst. North Pac. Fish. Hokkaido Univ.* **1977**, 175–197.
20. Nakatani, T. Studies on the early life history of walleye pollock *Theragra chalcogramma* in Funka Bay and vicinity, Hokkaido. *Mem. Fac. Fish. Hokkaido Univ.* **1988**, *35*, 1–46.
21. Nakatani, T. Year class strength and early life history of the Pacific population of walleye pollock, *Gadus chalcogrammus*, in Japan. *Mem. Fac. Fish. Sci. Hokkaido Univ.* **2016**, *58*, 1–11.
22. Nakatani, T.; Maeda, T. Early life history of walleye pollock. *Sci. Rep. Hokkaido Fish. Exp. Stat.* **1993**, *42*, 15–22.
23. Hashimoto, Y.; Maeda, A.; Oono, Y.; Kano, Y.; Takatsu, T. Feeding habits of two flatfish species larvae in Funka Bay, Japan: Importance of *Oikopleura* as prey. *Bull. Plankton Soc. Jpn.* **2011**, *58*, 165–177.
24. Nakatani, T. Relationship between hydrographic conditions in Funka Bay, Hokkaido, during winter and year class strength of the Japanese Pacific population of walleye pollock *Gadus chalcogrammus* from 1991 to 2013. *Mem. Fac. Fish. Sci. Hokkaido Univ.* **2017**, *59*, 19–43.
25. Ohtani, K. Studies on the change of the hydrographic conditions in the Funka Bay: II. Characteristics of the waters occupying the Funka Bay. *Bull. Fac. Fish. Hokkaido Univ.* **1971**, *22*, 58–66.
26. Ooki, A.; Shida, R.; Otsu, M.; Onishi, H.; Kobayashi, N.; Iida, T.; Nomura, D.; Suzuki, K.; Yamaoka, H.; Takatsu, T. Isoprene production in seawater of Funka Bay, Hokkaido, Japan. *J. Oceanogr.* **2019**, *75*, 485–501. [CrossRef]
27. Hirakawa, K. Seasonal change of population structure of a boreal oceanic copepod, *Eucalanus bungii bungii* Johnson in Funka Bay, Hokkaido, Japan. *Bull. Fac. Fish. Hokkaido Univ.* **1976**, *27*, 71–77.
28. Hirakawa, K. Seasonal change of population structure of a calanoid copepod, *Calanus pacificus*, in Funka Bay, Hokkaido. *Bull. Plankton Soc. Jpn.* **1979**, *26*, 49–58.
29. Hirakawa, K. Seasonal Distribution of the Planktonic Copepods, and Life Histories of *Calanus pacificus*, *Calanus plumchrus*, and *Eucalanus bungii bungii* in the Waters of Funka Bay, Southern Hokkaido, Japan. Ph.D. Thesis, Hokkaido University, Hokkaido, Japan, 1983.
30. Dohi, K. Seasonal change of tintinnid community in Funka Bay. *Bull. Plankton Soc. Jpn.* **1982**, *29*, 77–87.
31. Shiga, N. Seasonal and vertical distributions of Appendicularia in Volcano Bay, Hokkaido, Japan. *Bull. Mar. Sci.* **1985**, *37*, 425–439.
32. Yokouchi, K. Reproduction and larval ecology of the sandworm *Neanthes virens* (Sars) from southern Hokkaido. *Bull. Plankton Soc. Jpn.* **1985**, *32*, 1–13.
33. Yamaoka, H.; Takatsu, T.; Suzuki, K.; Kobayashi, N.; Ooki, A.; Nakaya, M. Annual and seasonal changes in the assemblage of planktonic copepods and appendicularians in Funka Bay before and after intrusion of Coastal Oyashio Water. *Fish. Sci.* **2019**, *85*, 1077–1087. [CrossRef]
34. Teraoka, T.; Amei, K.; Fukai, Y.; Matsuno, K.; Onishi, H.; Ooki, A.; Takatsu, T.; Yamaguchi, A. Seasonal changes in taxonomic, size composition, and normalised biomass size spectra (NBSS) of mesozooplankton communities in Funka Bay, southwestern Hokkaido: Insights from ZooScan analysis. *Plankton Benthos Res.* **2022**, *17*, 369–382. [CrossRef]
35. Kida, S.; Takayama, K.; Sasaki, Y.N.; Matsuura, H.; Hirose, N. Increasing trend in Japan Sea throughflow transport. *J. Oceanogr.* **2021**, *77*, 145–153. [CrossRef]
36. Abe, H.; Yahiro, Y.; Hasegawa, T.; Hirawake, T.; Onishi, H.; Ooki, A.; Takatsu, T.; Sasaki, K.; Wakita, M.; Kaneko, H.; et al. Intrusion of Coastal Oyashio water to Funka Bay and Tsugaru Strait occasionally disturbed by Kuroshio-originating warm core ring. *J. Oceanogr.* **2023**, *79*, 349–366. [CrossRef]

37. Kuroda, H.; Setou, T. Extensive marine heatwaves at the sea surface in the Northwestern Pacific Ocean in summer 2021. *Remote Sens.* **2021**, *13*, 3989. [CrossRef]
38. Welschmeyer, N.A. Fluorometric analysis of chlorophyll a in the presence of chlorophyll b and pheopigments. *Limnol. Oceanogr.* **1994**, *39*, 1985–1992. [CrossRef]
39. Miyaguchi, H.; Fujiki, T.; Kikuchi, T.; Kuwahara, V.S.; Toda, T. Relationship between the bloom of *Noctiluca scintillans* and environmental factors in the coastal waters of Sagami Bay, Japan. *J. Plankton Res.* **2006**, *28*, 313–324. [CrossRef]
40. Ara, K.; Nakamura, S.; Takahashi, R.; Shiomoto, A.; Hiromi, J. Seasonal variability of the red tide-forming heterotrophic dinoflagellate *Noctiluca scintillans* in the neritic area of Sagami Bay, Japan: Its role in the nutrient-environment and aquatic ecosystem. *Plankton Benthos Res.* **2013**, *8*, 9–30. [CrossRef]
41. Suzuki, T.; Yamamoto, K.; Narasaki, T. Predation pressure of *Noctiluca scintillans* on diatoms and thecate dinoflagellates off the western coast of Kyushu, Japan. *Plankton Benthos Res.* **2013**, *8*, 186–190. [CrossRef]
42. Onbé, T. Seasonal fluctuations in the abundance of populations of marine cladocerans and their resting eggs in the Inland Sea of Japan. *Mar. Biol.* **1985**, *87*, 83–88. [CrossRef]
43. Onbé, T.; Ikeda, T. Marine cladocerans in Toyama Bay, southern Japan Sea: Seasonal occurrence and day-night vertical distributions. *J. Plankton Res.* **1995**, *17*, 595–609. [CrossRef]
44. Iguchi, N.; Kidokoro, H. Horizontal distribution of *Thetys vagina* Tilesius (Tunicata, Thaliacea) in the Japan Sea during spring 2004. *J. Plankton Res.* **2006**, *28*, 537–541. [CrossRef]
45. Iguchi, N. Zooplankton in Toyama Bay, southern Japan Sea. *Bull. Coast. Oceanogr.* **2020**, *58*, 77–79.
46. Chiba, S.; Ono, T.; Tadokoro, K.; Midorikawa, T.; Saino, T. Increased stratification and decreased lower trophic level productivity in the Oyashio Region of the North Pacific: A 30-year retrospective study. *J. Oceanogr.* **2004**, *60*, 149–162. [CrossRef]
47. Tadokoro, K.; Chiba, S.; Ono, T.; Midorikawa, T.; Saino, T. Interannual variation in *Neocalanus* biomass in the Oyashio waters of the western North Pacific. *Fish. Oceanogr.* **2005**, *14*, 210–222. [CrossRef]
48. Kobari, T.; Tadokoro, K.; Sugisaki, H.; Itoh, H. Response of *Eucalanus bungii* to oceanographic conditions in the western subarctic Pacific Ocean: Retrospective analysis of the Odate Collections. *Deep-Sea Res. II* **2007**, *54*, 2748–2759. [CrossRef]
49. Fuji, T.; Nakayama, S.-I.; Hashimoto, M.; Miyamoto, H.; Kamimura, Y.; Furuichi, S.; Oshima, K.; Suyama, S. Biological interactions potentially alter the large-scale distribution pattern of the small pelagic fish, Pacific saury *Cololabis saira*. *Mar. Ecol. Prog. Ser.* **2023**, *704*, 99–117. [CrossRef]
50. Tian, Y.; Fu, C.; Yatsu, A.; Watanabe, Y.; Liu, Y.; Li, J.; Liu, D.; Pang, Y.; Cheng, J.; Ho, C.-H.; et al. Long-term variability in the fish assemblage around Japan over the last century and early warning signals of regime shifts. *Fish Fish.* **2023**, *24*, 675–694. [CrossRef]
51. Alldredge, A.L. Discarded appendicularian houses as sources of food, surface habitats, and particulate organic matter in planktonic environments. *Limnol. Oceanogr.* **1976**, *21*, 14–24. [CrossRef]
52. Flood, P.R. Architecture of, and water circulation and flow rate in, the house of the planktonic tunicate *Oikopleura labradoriensis*. *Mar. Biol.* **1991**, *111*, 95–111. [CrossRef]
53. Choe, N.; Deibel, D. Temporal and vertical distributions of three appendicularian species (Tunicata) in Conception Bay, Newfoundland. *J. Plankton Res.* **2008**, *30*, 969–979. [CrossRef]
54. Doubleday, A.J.; Hopcroft, R.R. Interannual patterns during spring and late summer of larvaceans and pteropods in the coastal Gulf of Alaska, and their relationship to pink salmon survival. *J. Plankton Res.* **2015**, *37*, 134–150. [CrossRef]
55. Miyamoto, T.; Takatsu, T.; Nakatani, T.; Maeda, T.; Takahashi, T. Distribution and food habits of eggs and larvae of *Hippoglossoides dubius* in Funka Bay and its offshore waters, Hokkaido. *Bull. Jpn. Soc. Fish. Oceanogr.* **1993**, *57*, 1–14.
56. Herman, A.W.; Harvey, M. Application of normalized biomass size spectra to laser optical plankton counter net intercomparisons of zooplankton distributions. *J. Geophys. Res.* **2006**, *111*, C05S05. [CrossRef]
57. Zhou, M.; Tande, K.S.; Zhu, Y.; Basedow, S. Productivity, trophic levels, and size spectra of zooplankton in northern Norwegian shelf regions. *Deep-Sea Res. II* **2009**, *56*, 1934–1944. [CrossRef]
58. Kudo, I.; Hisatoku, T.; Yoshimura, T.; Maita, Y. Primary productivity and nitrogen assimilation with identifying the contribution of urea in Funka Bay, Japan. *Estuar. Coast. Shelf Sci.* **2015**, *158*, 12–19. [CrossRef]